J Intell Robot Syst (2017) 86:199–211
DOI 10.1007/s10846-016-0417-1

Optimal Capture of a Tumbling Object in Orbit Using a Space Manipulator

Angel Flores-Abad · Lin Zhang · Zheng Wei · Ou Ma

Received: 14 February 2016 / Accepted: 1 September 2016 / Published online: 5 October 2016

Abstract This paper introduces an optimal capture strategy for a manipulator based on a servicing spacecraft to approach an arbitrarily rotating object, such as a malfunctioning satellite or a piece of orbital debris, for capturing with minimal impact to the robot's base spacecraft. The method consists of two steps. The first step is to determine an optimal future time and the target object's corresponding motion state for the robot to capture the tumbling object, so that, at the time when the gripper of the robot intercepts the target the very first instant, the resulting impact or disturbance to the attitude of the base spacecraft will be minimal. The second step is to control the robot to reach the tumbling object at the predicted optimal time along an optimal trajectory. The optimal control problem is solved with random uncertainties in the initial and final boundary conditions. Uncertainties are introduced because sensor and estimation errors inevitably exist in the first step, i.e., determination process of the initial and final boundary conditions. The application of the method is demonstrated using a dynamics simulation example.

Keywords Space robot · Optimal control · Capture · Tumbling target · Tumbling object · Minimal impact · Uncertainties

A. Flores-Abad (✉)
Mechanical Engineering Department, University of Texas at El Paso, El Paso, TX 79968, USA
e-mail: afloresabad@utep.edu

L. Zhang · O. Ma
Department of Mechanical and Aerospace Engineering, New Mexico State University, Las Cruces, NM 88003, USA

Z. Wei
Department of Mathematics and Statistics, University of Massachusetts Amherst, Amherst, MA 01002, USA

1 Introduction

Using manipulators mounted on a spacecraft for on-orbit services (OOS) of satellites is increasingly attracting the attention of the aerospace community. As a result, robotics-based OOS technologies have been significantly advanced in the past two decades [1]. However, capturing a non-cooperative object, such as an out-of-control satellite a tumbling asteroid, or a piece of tumbling space debris in space is still a very challenging and risky operation. One of the major problems encountered in a robotics-based OOS mission is the attitude disturbance to the base spacecraft caused by the physical interception between the robot and the target object, which may cause destabilization of the servicing spacecraft or severe damage to the interface hardware. Several approaches have been proposed to deal with this problem in the literature. Wee and Walker [2] studied the dynamics of contact between space robots and developed an algorithm to achieve both trajectory tracking and impulse minimization. Yoshida and Nenchev [3] introduced

the concept of Reaction-Null Space, to find out the best manipulator configuration for a safe capture with minimal impact force. Papadopoulos and Paraskevas [4] proposed a methodology based on the percussion point of bodies to minimize the forces transmitted to the base of the manipulator when grasping an object. Huang et al. [5], also found that the configuration of a manipulator at the contact moment is an important factor to consider in order to reduce the impact effect. Then, in reference [6], an optimal trajectory planning method for minimizing the impact is proposed. With the objective of minimizing or avoiding the impact effect, in reference [7] the authors used a genetic algorithm to search for an optimal configuration of a manipulator at the capturing instant. Thus, there will be minimal attitude change in both the final approaching phase and the capturing phase. To date, no one has demonstrated autonomous robotic capture of an object which had already rotated in orbit before the mission.

In this paper, we propose an approach to reduce or nullify the attitude disturbance on the base spacecraft at the capturing moment. The idea is first to predict the best capturing time and configuration such that the contact force resulting from the first physical contact passes through the center of mass of the whole servicing system (including both the servicing spacecraft and the robot). In this way, the attitude disturbance caused by the contact is zero or minimal. Then, an optimal control with uncertainties in the initial and final boundary conditions is developed to control the robot to reach the predicted location with a minimal attitude disturbance on the servicing spacecraft.

The problem of optimal trajectory planning for a space manipulator was addressed by a few researchers. Dubowsky and Torres [8] did some early and preliminary work. Agrawal and Xu [9] proposed a global optimum path planning for redundant space manipulators. Papadopoulos and Abu-Abed introduced a motion planning for a zero-reaction manipulator [10]. Lampariello et al. [11] presented an optimal motion planning method using criteria in the joint space. Aghili [12] designed an optimal controller to capture a tumbling satellite using an objective function minimizing the operation time and the relative velocity between the robot tip and the target. Oki et al. [13] also proposed an optimal control method to capture a tumbling satellite, but they focused mainly on minimizing the operational time for fast capturing.

Uncertainties in model parameters as well as in the measuring system are inevitable. To overcome the problem of unknown model parameters, several adaptive (see for example [14–16]) and robust controllers e.g. references [17–19] have been introduced. Besides, Chen and Chen [20] developed a robust adaptive approach to cope with uncertain parameters as well as with external disturbances. On the other hand, to account for uncertainties due to imperfection in measuring system, statistical approaches can be implemented, such as the case of the optimal controller for space robotics applications reported in [21]. In that work the author considered uncertainties only during the estimation of the target's parameters. However, the uncertainties were not considered in the optimal control solution for the motion planning of the manipulator. We proposed a control method which allows uncertainties in the initial and final boundary conditions of the optimal control problem [22]. In this paper, we apply this method to a full capture problem.

The optimal capture approach presented in this paper is different from the existing approaches in the following aspects: i) it does not require zero relative velocity between the end-effector and the grasping handle of the target object at the capturing moment, as the contact force direction will pass through the mass center of the servicing system; ii) the proposed cost function minimizes (not only constrains) the reaction torque at the root of the manipulator, which will reduce the base spacecraft attitude disturbance; iii) uncertainties are introduced in the manipulator's motion control scheme; and iv) minimization of servicing spacecraft's attitude disturbances is considered in the final robot approaching and at the capturing moment as well. In references [22, 23] the authors presented some earlier results of this research, where a fully-controlled base spacecraft (fixed-base) and a perfect measurement system (i.e., no uncertainties in the problem). These conditions are removed in the work reported in this paper.

The rest of the paper is organized as follows: In Section 2, the dynamic modeling of the servicing system and target object is presented. The determination of the optimal time and point to capture is described in Section 3. The formulation of the optimal controller with uncertainties is introduced in Section 4. The general approach is validated with a simulation example in Section 5 and finally the conclusions are given in Section 6.

2 Dynamic Modelling

2.1 Basis Assumptions

The development of the methodology described in this paper is based on the following basic assumptions:

1) Both the servicing spacecraft and the target object are assumed to be rigid bodies. The manipulator on the servicing spacecraft also consists of rigid links only.
2) The servicing spacecraft and the target object have been in proximity range and thus, the effect of orbital mechanics is neglected.
3) The external forces (including torques) which may exist in an orbit, such as the gravity gradient, air drag, magnetic force, and solar wind are expected to be insignificant in comparison to the robot's actuator forces, inertia forces, joint friction, and contact forces (during physical contact of capturing), and therefore are ignored.
4) The servicing system is assumed to be driftless, i.e., the initial angular momentum is zero.
5) The mass properties and the motion states of the servicing spacecraft and the target object are assumed to be known. However, errors in estimated motion states of the spacecraft and the target are allowed, which will be handled as the initial and final boundary conditions in Section 4.
6) In order for the contact force to be small and so prevent the damage of the servicing system, our method requires the close ranges rendezvous to be performed effectively, such that the difference between the capturing interfaces' velocities is small.

Assumptions (1) to (3) are a common treatment in the research area of space robotics for on-orbit services, for instance [2–23]. Assumption 4) is reasonable when the attitude of the servicing vehicle is well controlled and the orbital rotation is ignored under Assumption (2). For those readers interested in the effects of considering non-zero angular momentum, please see [24]. Assumption (5) allows us to focus our investigation in the dynamics and optimal control of the space manipulator. Studies of the determination or estimation of mass properties and motion state can be found in [25–29]. Regarding assumption (6), note that, in case the contact force is large, it will only produce a linear displacement, which should be negligible to the orbiting motion.

2.2 Kinematics

It is assumed that the robotic system of the servicing spacecraft including both the spacecraft and the manipulator consists of $n+1$ rigid bodies connected by n single-DOF (degree of freedom) joints, as shown in Fig. 1. Body 0 (or Link 0) is the servicing spacecraft which is also the base of the robot. Body i is the ith link of the manipulator. Joint 0 of the system has 6 DOF, which connects the inertial frame to the servicing spacecraft, and joint i is assumed to have only one DOF which articulates links i-1 and i. Unless otherwise specified, all the vectors are assumed to be expressed in the inertial frame F_0 which is originated at the mass center C_0 of the spacecraft. Moreover, F_1 is a frame attached to the spacecraft with its origin at Joint 1 and F_e is the end-effector frame rigidly attached to the end-effector.

In the introduced methodology the end-effector position and velocity must be known in order to determine if the capturing point has been reached. The position of the end-effector is defined as

$$\mathbf{r}_e = \mathbf{r}_0 + \mathbf{a}_0 + \sum_{i=1}^{n} \mathbf{a}_i \quad , \quad i = 1, 2, \cdots, n \tag{1}$$

where $\mathbf{r}_0 \in R^3$ and $\mathbf{r}_e \in R^3$ are the positions of the mass center C_0 of the spacecraft and the position of the end-effector of the manipulator with respect to the inertial frame F_0.; $\mathbf{a}_i \in R^3$ is the vector connecting the two connecting joints of the ith link of the manipulator.

By measuring the attitude and linear displacement of the base spacecraft, plus the robot's joint angles, the end effector position $\mathbf{r}_e$ can be known. Differentiating (1) with respect to time, the following relationship between the end-effector linear velocity and joint velocity is obtained

$$\mathbf{v}_e = \mathbf{v}_0 + \boldsymbol{\omega}_0 \times (\mathbf{r}_e - \mathbf{r}_0) + \sum_{i=1}^{n} \left[\mathbf{z}_i \times \left(\mathbf{r}_e - \boldsymbol{\rho}_i\right)\right]\dot{\theta}_i \tag{2}$$

where $\mathbf{v}_0 \in R^3$ and $\boldsymbol{\omega}_0 \in R^3$ are the linear and angular velocity vectors of the spacecraft, respectively; $\mathbf{v}_e \in R^3$ is the linear velocity vector of the end-effector of the manipulator; $\mathbf{z}_i \in R^3$ is the unit vector of the ith joint axis; $\boldsymbol{\rho}_i \in R^3$ is the position vector as defined

in Fig. 1; and θ_i is the joint angle of the ith joint. Besides, the end-effector angular velocity and the joint velocities are related by

$$\boldsymbol{\omega}_e = \boldsymbol{\omega}_0 + \sum_{i=1}^{n} \mathbf{z}_i \dot{\theta}_i \tag{3}$$

Assuming that there are no external forces acting on the servicing system, the momentum of the system will be conserved. The dynamics equations of the space robot including the servicing spacecraft can be derived in terms of its joint variables as follows [29]:

$$\mathbf{H}\ddot{\boldsymbol{\theta}} + \mathbf{C}\dot{\boldsymbol{\theta}} = \boldsymbol{\tau}, \tag{4}$$

where $\boldsymbol{\theta} \in R^n$ is the generalized joint coordinates and

$$\mathbf{C}\dot{\boldsymbol{\theta}} = -\frac{\partial}{\partial \boldsymbol{\theta}} \left\{ \frac{1}{2} \dot{\boldsymbol{\theta}}^T \mathbf{H} \dot{\boldsymbol{\theta}} \right\} \in R^n, \tag{5}$$

which represents the nonlinear Coriolis and centrifugal forces acting on the system and $\mathbf{H} \in R^{n\times n}$ is the generalized inertia matrix of the manipulator. When the robot is attached to a free-floating base, $\mathbf{H}$ can be derived to be

$$\mathbf{H} = \mathbf{H}_\theta - \begin{bmatrix} \mathbf{J}_{m0}^T & \mathbf{H}_{\omega\theta}^T \end{bmatrix} \begin{bmatrix} m\mathbf{1} & m\mathbf{R}_{0c}^T \\ m\mathbf{R}_{0c} & \mathbf{H}_\omega \end{bmatrix}^{-1} \begin{bmatrix} \mathbf{J}_{m0} \\ \mathbf{H}_{\omega\theta} \end{bmatrix}, \tag{6}$$

where

$$\mathbf{H}_\theta = \sum_{i-1}^{2} \left(\mathbf{J}_{\omega i}^T \mathbf{I}_i \mathbf{J}_{\omega i} \right) \in R^{n\times n}$$

$$\mathbf{J}_{\omega i} = [\mathbf{z}_1 \quad \mathbf{z}_2 \quad \cdots \quad \mathbf{z}_i \quad 0 \quad \cdots] \in R^{3\times n}$$

$$\mathbf{J}_{vi} = [\mathbf{z}_1 \times \boldsymbol{\rho}_{c1} \quad \mathbf{z}_2 \times \rho_i \times \boldsymbol{\rho}_{ci} \quad 0 \quad \cdots] \in R^{3\times n}$$

$$\mathbf{J}_{m0} = \sum_{i=1}^{n} m_i \mathbf{J}_{vi} \in R^{3\times n}$$

$$\mathbf{H}_{\omega 0} = \sum_{i=1}^{n} (\mathbf{I}_i \mathbf{J}_{\omega i} + m_i \mathbf{Z}_i \mathbf{J}_{vi}) \in R^{3\times n}$$

$$\mathbf{Z}_i = \begin{bmatrix} 0 & -z_i(3) & z_i(2) \\ z_i(3) & 0 & -z_i 1 \\ -z_i(2) & z_i 1 & 0 \end{bmatrix} \in R^{3\times 3} \text{ for any vector } \mathbf{z}$$

$$\mathbf{H}_\omega = \left(\sum_{i=1}^{n} \mathbf{I}_i + m_i \mathbf{r}_{0i}^T \mathbf{r}_{0i} \right) + \mathbf{I}_0 \in R^{3\times 3}$$

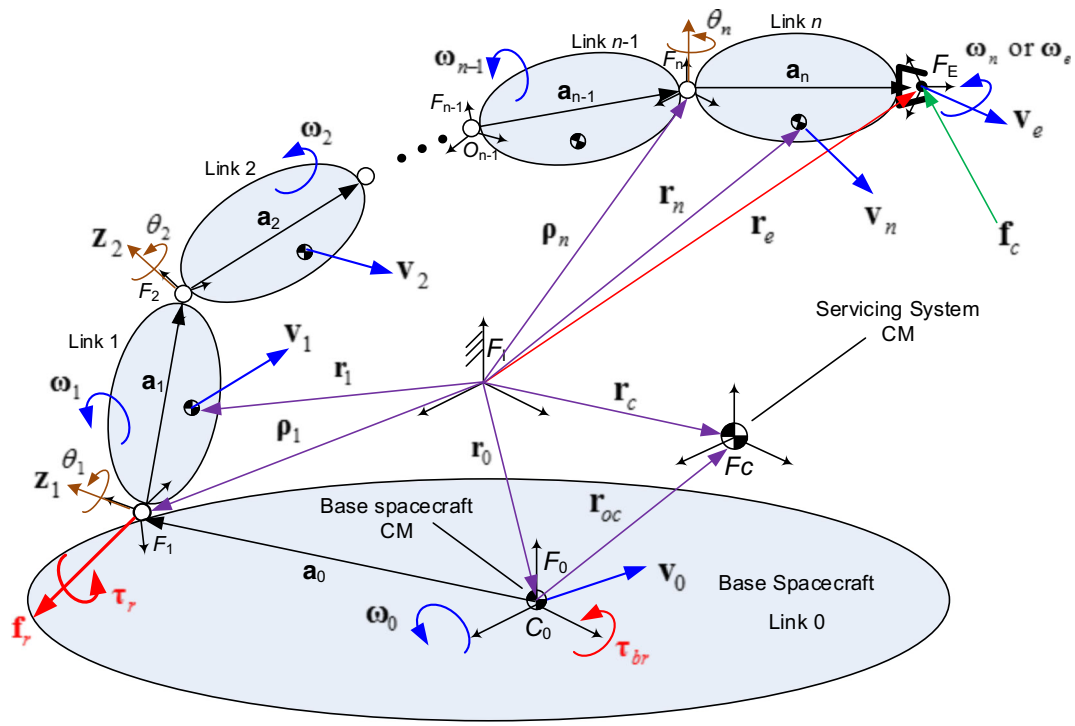

Fig. 1 Multibody dynamic system of a servicing spacecraft with an onboard manipulator

Further, m_i is the mass of the ith link of the manipulator; m is the total mass of servicing spacecraft and the robot; $\mathbf{R}_{0c} \in^{3\times3}$ is the skew symmetric matrix of the vector $\mathbf{r}_{0c} = \mathbf{r}_c - \mathbf{r}_0 \in R^3$; $\mathbf{R}_{0i} \in^{3\times3}$ is the skew symmetric matrix of the vector $\mathbf{r}_{0i} = \mathbf{r}_i - \mathbf{r}_0 \in R^3$; $\mathbf{1} \in R^{3\times3}$ is an identity matrix with the indicated dimensions ;$\boldsymbol{\rho}_{ci} \in R^3$ is the position vector from the $i-$th joint to the tip of the robot; $\mathbf{I}_i \in R^{3\times3}$ is the centroidal inertia matrix of the ith link of the robot; and $\mathbf{I}_0 \in R^{3\times3}$ is the centroidal inertia matix of the servicing spacecraft. In this work, the ReDySim [30] floating-base module, was used to generate the dynamics model of the servicing system based on Eqs. 4–6 and the SimMechanics™ of Matlab/Simulink® was used to run the simulations.

2.3 Dynamics Modeling of the Target Object

Since the target object is assumed to be a single rotating rigid body, its dynamics equation in body frame is given by,

$$\mathbf{I}_t\dot{\boldsymbol{\omega}}_t + \boldsymbol{\omega}_t \times \boldsymbol{I}_t\, \boldsymbol{\omega}_t = \boldsymbol{\tau}_t, \tag{7}$$

where

$\mathbf{I}_t \in R^{3\times3}$: inertia matrix of the target satellite.
$\boldsymbol{\omega}_t \in R^3$: angular velocity of the target satellite.
$\dot{\boldsymbol{\omega}}_t \in R^3$: angular acceleration of the target satellite.
$\boldsymbol{\tau}_t \in R^3$: external torque applied to the target satellite.

The external torque vector $\boldsymbol{\tau}_t \in R^3$ is zero without physical contact at the robot's gripper and it is the contact torque during a capture or gasping operation.

3 Determination of the Optimal Time and Configuration of the Target to Capture

As stated earlier, the overall goal for the control design is to capture a tumbling object with minimal impact on the attitude motion of the servicing spacecraft. The first step for achieving such a goal is to determine a best time and configuration of the target for the robot to grasp. It is understandable that if the resultant contact force exerted at the robot tip (resulting from a capture action) passes the mass center of the servicing system, the contact force will not cause any attitude disturbance to the servicing spacecraft, as shown in Fig. 2.

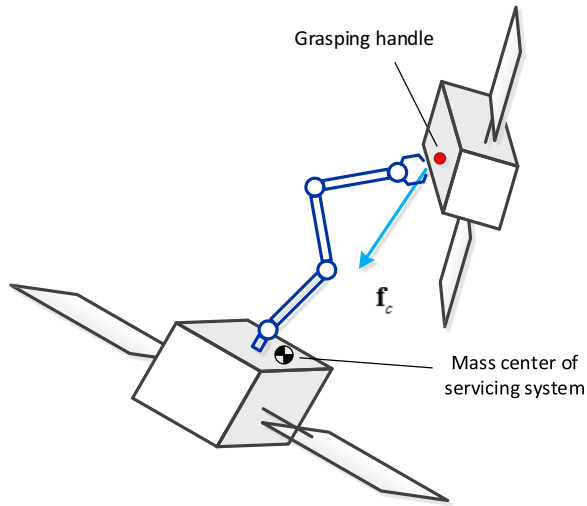

Fig. 2 Interception for minimal impact to the base satellite based on the contact force direction.

However, the direction of contact force depends on the relative velocity, contacting spots and contact geometry, which makes it very difficult to predict in advance. Although, such a prediction may not be impossible if we have an accurate contact dynamics model available, this will require more research work in the future. For this work, we approximate it by assuming that the contact force is approximately along the direction of the relative velocity between the robot tip and the grasping point of the target object. Therefore, no attitude disturbance to the servicing spacecraft can be achieved by either of the following two conditions:

1) The relative velocity between the robot tip and the grasping point of the target object is zero.
2) The relative velocity between the robot tip and the grasping point of the target object is nonzero, but its direction passes through the mass center of the servicing system.

The design of control strategies to meet the first condition is a common approach, such as the work described in[21]. It requires that the robot tip must move as fast as the grasping point of the tumbling object. This is very difficult or even impossible when the target object has a fast tumbling motion because the tip speed of a manipulator is always limited not only by the joint rate and torque limits, but also by the attitude tolerance of the servicing spacecraft, because when

the onboard robot move too fast the base spacecraft may not always be able to control its attitude. In such a case, a strategy using the second condition as its control goal becomes more attractive because it does not require zero relative velocity, but such an approach has not been studied in the past. Therefore, we will focus our study on achieving the second condition.

As shown in Fig. 3, the above-mentioned second condition means that the angle β (between the relative velocity and the position vector of the grasped point of the target object) should be zero. In such a case, the major component of the impact force (assuming mainly along the relative velocity direction) will pass through the mass center of the servicing spacecraft system and thus, cause no angular moment to the servicing spacecraft.

Of course, this is only an ideal case. In a general tumbling case, the direction of the relative velocity may never pass through the mass center of the servicing spacecraft system. However, even if the angle β can never reach zero, it will reach a minimal value at some time and thus, result in minimal attitude disturbance to the base spacecraft. Hence, we will just focus on the problem to determine such a minimal angle. This can be formulated as: given a set of initial motion conditions of the target object, find a future time such that the angle between the relative velocity and position vector of the grasped point of the target will be zero or minimum. Mathematically, this can be expressed as

$$t_1 = \arg\max_t \cos\beta = \arg\max_t \frac{\mathbf{v}(t)\cdot\mathbf{r}(t)}{\|\mathbf{v}(t)\|\,\|\mathbf{r}(t)\|}, \quad (8)$$

where

$$\mathbf{v}(t) = \mathbf{v}_t + \mathbf{R}(\boldsymbol{\omega}_t \times \mathbf{a}), \quad \mathbf{r}(t) = \mathbf{r}_{ct} + \mathbf{R}\mathbf{a} \quad (9)$$

In the above problem definition, $\mathbf{R} \in R^{3\times3}$ is the rotation matrix defining orientation of the target object frame F_t with respect to the frame F_0. Position vector $\mathbf{a} \in R^3$ points to the grasped point from the mass center of the target object, expressed in the object's body-fixed frame F_t. $\mathbf{R}(t)$ and $\boldsymbol{\omega}_t(t)$ can be solved from Eq. 7 numerically with the known initial conditions, which is just a common forward dynamics problem. It should be pointed out that there exists a possibility that the optimization problem (8) does not have a solution (i.e., a singular case) when the grasping point is on the rotation axis. In such a case velocity v(t) is constant and thus, there is no minimal solution for angle β. However, this is a degenerated case and very easy to handle because the rotation of the target is no longer affecting the relative velocity between the robot's tip and the target's grasping point from the initial time.

Considering the case without external forces and torques acting on the target object, the rotation of an

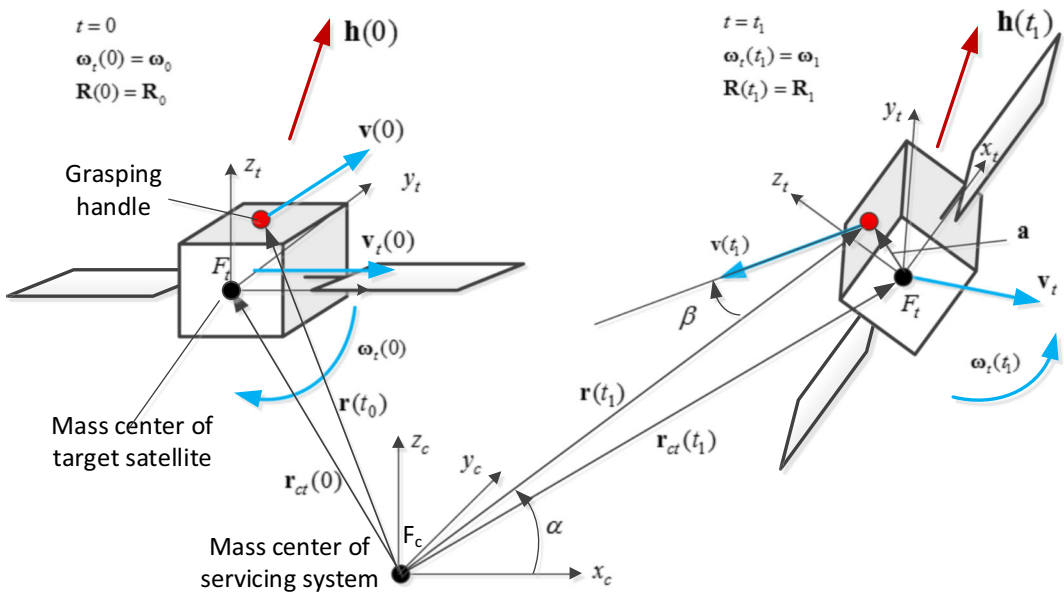

Fig. 3 The initial configuration (*left*) and the intercepting configuration (*right*) of the target object

object is periodic in the body-fixed frame but can be either periodic or quasiperiodic in an inertial frame. The motion is periodic in an inertial frame if the object is spinning in one of the principal axes or rotating even with precession. On the other hand, if the object is tumbling, the attitude changing is still quasiperiodic in an inertial frame, i.e. "almost periodic," because in this scenario, the orientation is function of more than one frequency, which in some cases are incommensurable [31]. In this work we assume that the target object is rotating periodically. Thus, we expect that the optimal capture opportunity discussed above will be repeated. This means that we can have enough time to prepare for a safe and optimal motion trajectory for the robot, because the desired capture time and opportunity will come repeatedly over the time. Of course, in reality, the target will unlikely be doing perfectly periodic rotation also because there could exist some non-zero external forces and moments as well as small damping in the target object. Therefore, the tumbling motion may not be kept periodic just as the case discussed in [32], where gravity gradient is considered. However, as long as such changing of motion behavior is relatively slow in time, we will still have time to plan and perform an optimal capture task, as described in the next section.

4 Optimal Control for the Robot's Approaching with Uncertainties on the Boundary Conditions

Once an optimal future time for capturing is determined, the corresponding motion state of the target object can also be predicted. This optimal time and motion state will be used as the final time and reference pose of the end-effector for developing the control of the robot to perform the capture task. To focus on the robotics control, it is assumed that the servicing spacecraft has been controlled to keep a fixed distance to the target object (that is, on a station keeping mode) such that the target object is within the reach of the robotic arm.

To develop the optimal control, the robot's dynamics equation (4) is rewritten into a state space form as follows

$$\dot{\mathbf{x}} = \mathbf{f}(\mathbf{x}) + \mathbf{G}(\mathbf{x})\boldsymbol{\tau}, \tag{10}$$

where $\mathbf{x} \in R^{2n}$ is the state vector; $\mathbf{f}(\mathbf{x}) \in R^{2n}$ is the state function, $\mathbf{G}(\mathbf{x}) \in R^{2n\times n}$ is the control matrix; and $\boldsymbol{\tau} \in R^n$ is the vector joint control torques. They are defined as

$$\begin{aligned} \mathbf{x} &= \begin{bmatrix} \mathbf{x_1} \\ \mathbf{x_2} \end{bmatrix} = \begin{bmatrix} \boldsymbol{\theta} \\ \boldsymbol{\tau} \end{bmatrix}, \\ \mathbf{f}(\mathbf{x}) &= \begin{bmatrix} \mathbf{0} & \mathbf{1} \\ \mathbf{0} & -\mathbf{H}(\mathbf{x}_1)^{-1}\mathbf{C}(\mathbf{x}) \end{bmatrix} \begin{bmatrix} \mathbf{x_1} \\ \mathbf{x_2} \end{bmatrix}, \\ \mathbf{G}(\mathbf{x}) &= \begin{bmatrix} \mathbf{0} \\ \mathbf{H}(\mathbf{x}_1)^{-1} \end{bmatrix} \end{aligned} \tag{11}$$

We can find the impact of the robot motion to the servicing spacecraft by deriving the reaction force and moment (see Fig. 1) on the root of the robot (at the first robot joint), namely,

$$\begin{bmatrix} \mathbf{f}_r \\ \boldsymbol{\tau}_r \end{bmatrix} = \begin{bmatrix} -\sum_{i=1}^{n} m_i \dot{\mathbf{v}}_i \\ -\sum_{i=1}^{n} \left(\mathbf{I}_{ci}\dot{\boldsymbol{\omega}}_i + (\mathbf{r}_i - \mathbf{a}_0) \times m_i \dot{\mathbf{v}}_i\right) \end{bmatrix}, \tag{12}$$

where $\mathbf{f}_r \in R^3$ and $\boldsymbol{\tau}_r \in R^3$ are the force and moment the robot applies at the its root, respectively. Therefore, the total reaction force $\mathbf{f}_{br} \in R^3$ and moment $\boldsymbol{\tau}_{br} \in R^3$ caused by the robot motion at the mass center of the servicing spacecraft are

$$\begin{bmatrix} \mathbf{f}_{br} \\ \boldsymbol{\tau}_{br} \end{bmatrix} = \begin{bmatrix} -\sum_{i=0}^{n} m_i \dot{\mathbf{v}}_i \\ -\sum_{i=0}^{n} \left(\mathbf{I}_{ci}\dot{\boldsymbol{\omega}}_i + m_i \mathbf{R}_i \dot{\mathbf{v}}_i\right) \end{bmatrix} \tag{13}$$

where $\mathbf{R}_i$ is the skew-symmetric matrix of the position vector $\mathbf{r}_i$. Our control goal is then to find a time history of each joint's control torque such that, when the manipulator's tip is controlled by this set of joint torques to move from its initial pose to its final pose, it will have minimal attitude disturbance to the servicing spacecraft. To find this set of optimal control torques, we can define the following objective function

$$\begin{aligned} J = \int_0^{t_f} \boldsymbol{\tau}_r^T \boldsymbol{\tau}_r dt, \mathbf{x}(t_0) = \mathbf{x}_0 &= \begin{bmatrix} \boldsymbol{\theta}_0 \\ \dot{\boldsymbol{\theta}}_0 \end{bmatrix}, \\ \mathbf{x}(t_f) = \mathbf{x}_f &= \begin{bmatrix} \boldsymbol{\theta}_f \\ \dot{\boldsymbol{\theta}}_f \end{bmatrix} \end{aligned} \tag{14}$$

For this optimal control problem, the initial state $\mathbf{x}_0$ is known and the final time t_f and the final state $\mathbf{x}_f$ are determined by solving the constrained optimization problem described in Section 3. In other words, it is a fixed time and fixed boundary problem. Note that the fixed boundary at the final time means a fixed reference pose of the end-effector solved from Eqs. 7 and 9

rather than fixed final joint angles of the robot which are not fixed because of the floating base. The joint angles can be calculated at any time using the generalized inverse kinematics of the servicing spacecraft system as described in Section 2.

In order to formulate the optimal control problem, let's define the Hamiltonian for the system as

$$H = H(\mathbf{x}, \boldsymbol{\lambda}, \boldsymbol{\tau}) = \lambda_0 \boldsymbol{\tau}_0^T \boldsymbol{\tau}_0 + \boldsymbol{\lambda}^T (\mathbf{f} + \mathbf{G}\boldsymbol{\tau}) \tag{15}$$

where $\boldsymbol{\lambda} \in R^{2n}$ is the vector of costate variables and $\lambda_0(t) =$ constant. In accordance with the optimal control theory [33], the maximum principle states that a necessary condition for an optimal control to minimize (14) requires the existence of a nonzero vector $\boldsymbol{\lambda} = (\lambda_0, \lambda_1, \cdots, \lambda_{2n})$ satisfying

$$\dot{\lambda} = -\frac{\partial H}{\partial \mathbf{x}} \tag{16}$$

Furthermore, since $H = H(\mathbf{x}, \boldsymbol{\lambda}, \boldsymbol{\tau})$ attains its maximum with respect to the nominal optimal control $\boldsymbol{\tau} = \tilde{\boldsymbol{\tau}}$, the first-order and second-order necessary conditions should be [33]

$$\frac{\partial H}{\partial \boldsymbol{\tau}} = \mathbf{0}, \quad \frac{\partial^2 H}{\partial \boldsymbol{\tau}^2} \leq \mathbf{0} \tag{17}$$

Then, we can get a nominal optimal solution $\tilde{\boldsymbol{\tau}} = \boldsymbol{\Lambda}^{-1}(\tilde{\mathbf{x}})$, where $\tilde{\mathbf{x}}$ is the associated optimal trajectory connecting the nominal boundary conditions $\mathbf{x}_0$ and $\mathbf{x}_f$, and $\boldsymbol{\Lambda}^{-1}$ is the inverse dynamics function of the servicing system. Since the dynamic equation (10) is nonlinear, $\tilde{\boldsymbol{\tau}}$ is obtained numerically and the associated optimal trajectory has the form of $\tilde{\mathbf{x}} = \phi(t : \mathbf{x}_0, \mathbf{x}_f), 0 \leq t \leq t_f$.

However, in reality the initial and final boundary values are not exactly known because of possible random errors in the sensing systems and the models used to determine the initial and final boundary conditions. Therefore, in order to include the effect of random initial and final end-effector positions, we consider $\mathbf{r}_e(t_0) = \mathbf{r}_{e0}$ and $\mathbf{r}_e(t_f) = \mathbf{r}_{ef}$ to be random vectors given by $\hat{\mathbf{r}}_{e0} = \mathbf{r}_{e0} + \boldsymbol{\varepsilon}_0$ and $\hat{\mathbf{r}}_{ef} = \mathbf{r}_{ef} + \boldsymbol{\varepsilon}_f$, here $\boldsymbol{\varepsilon}_0$ and $\boldsymbol{\varepsilon}_f$ are assumed to be independent, $\boldsymbol{\varepsilon}_0 \sim N_n(\mathbf{0}, \sum_0)$ and $\boldsymbol{\varepsilon}_f \sim N_n\left(\mathbf{0}, \sum_f\right)$, where N_n is the normal distribution with mean vector $\mathbf{0} \in R^n$ and covariance matrices $\sum_0 \in R^{n\times n}$ and $\sum_f \in R^{n\times n}$. Since the nominal optimal trajectory $\tilde{\mathbf{x}}$ is a function of end-effector positions, namely, $\tilde{\mathbf{x}} = \boldsymbol{\Gamma}^{-1}(\mathbf{r}_e)$, where $\boldsymbol{\Gamma}^{-1}$ denotes the inverse kinematics function of the robot, we have $\mathbf{x}_0 = \Gamma^{-1}(\mathbf{r}_{e0})$ and $\mathbf{x}_f = \Gamma^{-1}(\mathbf{r}_{ef})$, consequently

$$\tilde{\mathbf{x}} = \phi(t : \mathbf{x}_0, \mathbf{x}_f) = \phi\left(t : \Gamma^{-1}(\mathbf{r}_{e0}), \Gamma^{-1}(\mathbf{r}_{ef})\right) \tag{18}$$

Hence, in the stochastic situation, the optimal trajectory $\tilde{\mathbf{x}}$ becomes a function of the random vector, i.e. $\tilde{\mathbf{x}}(\hat{\mathbf{r}}_{e0}, \hat{\mathbf{r}}_{ef})$. Thus, we will take the expected value of the admissible trajectory $E\left[\tilde{\mathbf{x}}(\hat{\mathbf{r}}_{e0}, \hat{\mathbf{r}}_{ef})\right]$ to be our new optimal trajectory $\mathbf{x}^*$, which is given by

$$\mathbf{x}^* = \mathrm{E}\left[\tilde{\mathbf{x}}(\hat{\mathbf{r}}_{e0}, \hat{\mathbf{r}}_{ef})\right] = \iint \tilde{\mathbf{x}}(r_{e0}, r_{ef}) dF(r_{e0}, r_{ef}), \tag{19}$$

where $F(r_{e0}, r_{ef})$ is the joint probability distribution function of $\hat{\mathbf{r}}_{e0}$ and $\hat{\mathbf{r}}_{ef}$. To solve this problem, we apply the Markov Chain Monte Carlo (MCMC) method [34] to approximate the expectation (19). Particularly, we are using a Metropolis-Hasting algorithm, which is a general computational approach that replaces analytic integration by summation over samples generated from the iterative algorithms; therefore, Eq. 19 can be approximated by

$$\frac{1}{\eta}\sum_{k=1}^{\eta} \phi\left(t : \mathbf{r}_{e0}^{(k)}, \mathbf{r}_{ef}^{(k)}\right) \to_{\eta\to\infty} \mathbf{x}^* = E\left[\tilde{\mathbf{x}}(\hat{\mathbf{r}}_{e0}, \hat{\mathbf{r}}_{ef})\right], \tag{20}$$

where $\left\{\mathbf{r}_{e0}^{(k)}, \mathbf{r}_{ef}^{(k)}\right\}_{k=1}^{\eta}$ are independent samples distributed of $\left[\hat{\mathbf{r}}_{e0}^T, \hat{\mathbf{r}}_{ef}^T\right]^T$. Finally, by inverse dynamics and direct kinematics, we can obtain the optimal control law $\boldsymbol{\tau}^* = \boldsymbol{\Lambda}^{-1}(\mathbf{x}^*)$ and the end-effector position $\mathbf{r}_e^* = \boldsymbol{\Gamma}(\mathbf{x}^*)$, respectively.

5 Simulation Example

To show the application of the proposed optimal control strategy for capturing a tumbling object with uncertainties in the initial and final boundary conditions, we present an example using a planar manipulator to capture a tumbling object in this section. The base satellite has 3-DOF (two translational and one rotational), while the manipulator is a 2-DOF arm. The assumed mass and inertia parameter ratios are similar to those of the Orbital Express Mission [35], and are defined in Fig. 4 and Table 1.

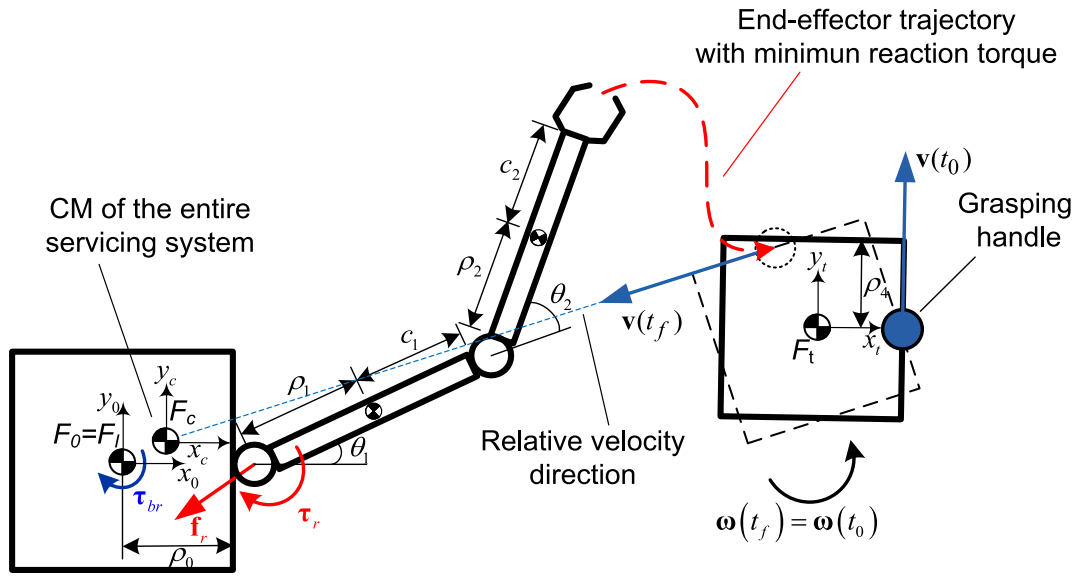

Fig. 4 Example of a 2-DOF free-floating space manipulator approaching a square target for capturing

In this simulation scenario we have set the inertial frame F_i coincident with the frame at the center of mass (COM) of the base spacecraft F_0 at $t = t_0$. Another reference frame F_t has been attached to the COM of the target object. Our proposed methodology is based on the fact that the direction of the relative velocity between the target object and the end-effector of the manipulator passes through the COM of the servicing system. This specification can be achieved in different manners, in this simulation example we consider the case where the robot manipulator reaches the target point at zero velocity (i.e., $\mathbf{v}_e = \boldsymbol{\omega}_e = 0$); thus, the relative velocity is only the velocity of the capturing spot in the target object.

5.1 Determination of the Optimal Time and State

In the final approaching phase, the space manipulator has already been unfolded from the stowed position and is deployed in a chaser configuration. Therefore, the initial state of the robotic arm is arbitrarily proposed to be as shown in Fig. 4, where $\theta_1(t_0) = \pi/6$rad and $\theta_2(t_0) = \pi/4$ rad, then, the end-effector position in inertial frame is $\mathbf{r}_{e0} = \begin{bmatrix} 1.625 & 1.466 \end{bmatrix}^T$ m. Under the absence of external forces and regardless the motion of the manipulator, the COM of the entire servicing system remains stationary for the entire maneuver at

$$\mathbf{r}_c = \frac{1}{m}\sum_{i=0}^{n} m_i \mathbf{r}_i = \begin{bmatrix} 0.05228 & 0.268 \end{bmatrix}^T \text{ m}.$$

The initial conditions of the target object (see Figs. 3 and 4) are assumed to be

$$\mathbf{R}(t_0) = \begin{bmatrix} 0 & -1 \\ 1 & 0 \end{bmatrix}, \ \mathbf{r}(t_0) = [1.625 \quad 1.466]^T \text{ m},$$
$$\boldsymbol{\omega}_t(t_0) = 0.541 \text{ rad/sec and } \mathbf{v}(t_0) = \begin{bmatrix} 0 & 0.2705 \end{bmatrix}^T \text{ m/s}$$

In the 2-D case, the rotational motion is simple and thus, using (8) and (9) we can easily find the optimal

Table 1 Parameters of the example space manipulator

Body	Bodynumber	(m)	(m)	(Kg)	(Kg m^2)
Base satellite	0	0.5	—	1100 (fueled)	25
Robot link 1	1	0.5	0.5	25	2.5
Robot link 2	2	0.5	0.5	25	2.5
Target satellite	4	0.5	—	225	18

time $t_f = 4s$ and the pose for the robot to reach for zero attitude-impact capture as

$$\mathbf{R}\left(t_f\right) = \begin{bmatrix} 0.2580 & 0.9662 \\ -0.9662 & 0.2580 \end{bmatrix} \text{ and}$$

$$\mathbf{r}(t_f) = \begin{bmatrix} 2.22 & 1.0 \end{bmatrix}^T \text{ m.} \quad (21)$$

5.2 Nominal Optimal Control Setup

Minimize:	$J(\mathbf{x}, \dot{\mathbf{x}}, \boldsymbol{\tau}) = \int_0^{tf} \boldsymbol{\tau}_r^T \boldsymbol{\tau}_r dt$
Subject to:	
−Dynamic Constraints:	Equation (10)
−Kinematics boundary constraints:	$\mathbf{r}_{e0} = [1.625 \quad 1.466]^T$ m
	$\mathbf{r}_{ef} = [2.22 \quad 1.0]^T$ m
	$\dot{\mathbf{r}}_{e0} = [0 \quad 0]^T$ m/s
	$\dot{\mathbf{r}}_{ef} = [0 \quad 0]^T$ m/s
−Final time:	$t_f = 4s$
−Box constraints:	$-3\text{Nm} \leq \tau_1 \leq 3\text{Nm}$
	$-3\text{Nm} \leq \tau_2 \leq 3\text{Nm}$
	$-\pi/2\text{rad} \leq \theta_1 \leq \pi/2\text{rad}$
	$-\pi/2\text{rad} \leq \theta_2 \leq \pi/2\text{rad}$

To solve the defined optimal control problem, we have used TOMLAB™, which utilizes a Gauss pseudospectral collocation method with Gaussian points as collocation points [36].

5.3 Optimal Control with Uncertainties in Boundary Conditions

With the objective of verifying the capability of the proposed method to deal with uncertainties in boundary conditions, a scenario with position sensor errors of ±2 cm is analyzed. Metropolis-Hasting MCMC method is used to get independent samples from a multivariate normal distribution with mean

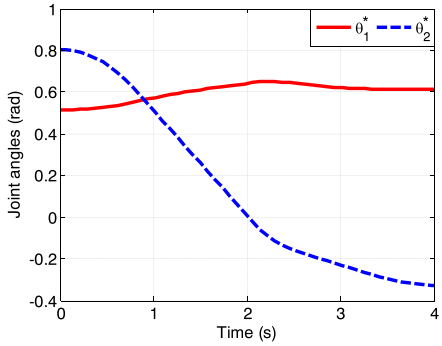

Fig. 5 Joint trajectories of the manipulator, where $\theta_1^*(t_0) = 0.53\text{rad}$, $\theta_2^*(t_0) = 0.778\text{rad}$, $\theta_1^*\left(t_f\right) = 0.615\text{rad}$ and $\theta_2^*(t_0) = -0.326\text{rad}$

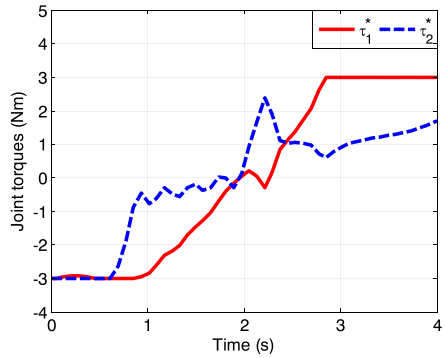

Fig. 6 Joint control torques with limits

$\mu = \begin{bmatrix} \mu_0^T & \mu_f^T \end{bmatrix}^T$, where $\mu_0^T = \begin{bmatrix} 1.625 & 1.466 \end{bmatrix}$ m and $\mu_f^T = \begin{bmatrix} 2.22 & 1.0 \end{bmatrix}$ m. The covariance matrix is defined as $\mathbf{P} = \text{diag}\left(\sum_0, \sum_f\right)$ with $\sum_0 = \sum_f = \text{diag}(0.0004, 0.0004)$.

The simulation example was run in a laptop computer with a core i7, 6GB in RAM and Windows 7 operating system. In the MCMC process, the simulation was run 1000 times for determining the control distance and compositing the numerical PDF (Probably Density Function). The whole computational process took 73 minutes. Note this inefficient computational speed was due to several contributing factors including using Tomlab software and Matlab script code. The speed could be drastically improved if we coded everything in C without using the general commercial software tools. In addition, more sophisticated computational algorithms can be utilized, such as the hybrid Monte Carlo Method or an over-relaxation algorithm [37] to avoid random walks. However, address of the computational efficiency will be one of our future research efforts.

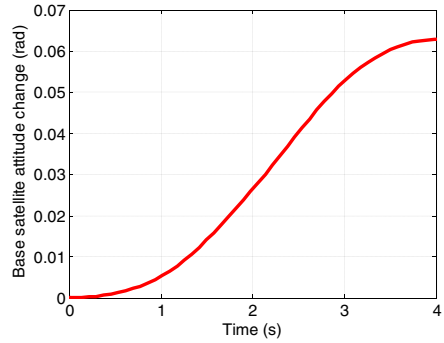

Fig. 7 Attitude change of the base spacecraft

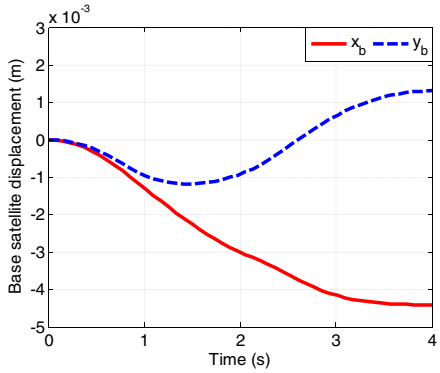

Fig. 8 Linear motion of the base spacecraft

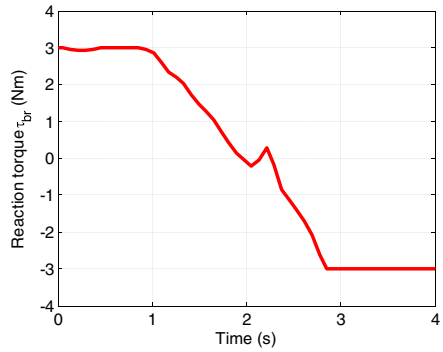

Fig. 10 Reaction torque $\boldsymbol{\tau}_{br}$ at the COM of the base spacecraft

Figure 5 shows the optimal trajectory of the states $\mathbf{x}^* = \left[\theta_1^* \ \theta_2^*\right]^T$ and Fig. 6 the associated optimal control torques $\boldsymbol{\tau}^* = \left[\tau_1^* \ \tau_2^*\right]^T$, where only τ_1^* reaches the upper and lower limits. On the other hand, as expected, the manipulator motion will cause the base spacecraft to rotate and translate. However, here the reaction torque $\boldsymbol{\tau}_{br}$ produced by the manipulators motion on the COM of base spacecraft was minimized; therefore, as depicted in Fig. 7, the maximum attitude change is very small (0.062 rad).

In the introduced optimal capture strategy, the cost function is intended to minimize the reaction torque on the base spacecraft with the objective of avoiding a big attitude change due to the manipulator's motion. However, the reaction force will cause the spacecraft to translate as depicted in Fig. 8. Nevertheless, this linear displacement is also very small and does not represent a major concern because the translation of the base will be just a small delta to the existing orbiting motion.

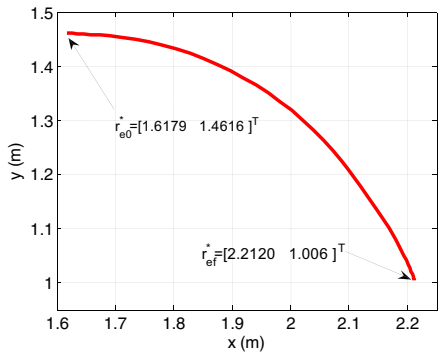

Fig. 9 XY plot of the end-effector trajectory

Despite the base spacecraft's rotation and translation, and the uncertainties in the boundary conditions, it can be observed in Fig. 9 that the robot practically reaches the desired capturing point at the desired instant, because the end-effector position vector $\mathbf{r}_{ef}^* = \left[1.6179 \ 1.4614\right]^T$m resulting from the random process is very close to the nominal vector. The corresponding initial end-effector position is $\mathbf{r}_{e0}^* = \left[2.2120 \ 1.006\right]^T$ m. The difference between the nominal final position $\mathbf{r}_{ef}$ and actual position $\mathbf{r}_{ef}^*$ at the impact moment is very small given by $\mathbf{e}_f = \left|\mathbf{r}_{ef} - \mathbf{r}_{ef}^*\right| = \left[0.008 \ 0.006\right] m$. It is also worth mentioning that in order to control the robot to reach the target position, only the manipulator's joints are actuated. However, in this work, the end-effector position is computed using (1), which requires measuring the attitude change and linear displacement of the base spacecraft. The reaction torque at the COM of the base spacecraft, is shown in Fig. 10.

6 Conclusions

An optimal control strategy for a space manipulator to reach a tumbling object for capture with uncertainties in the initial and final boundary conditions were presented. The objective of the strategy is to minimize the attitude disturbance applied to the base satellite due to the robot's approaching motion and the initial physical interception with the tumbling target object. The control strategy consists of two steps. In the first step, an optimal future time and the corresponding target pose of the tumbling object for the robot to capture are determined by a constrained nonlinear

optimization procedure. In the second step, an optimal controller is designed for the space robot to reach the targeted pose at the optimal time while exerting a minimal reaction torque on the base satellite. This means that the robot will cause minimal attitude disturbance to the base satellite during the capture process, including its maneuvering from the initial pose to the final pose and the very first contact to the target object. Random errors due to the uncertainties in the initial and final boundary conditions are considered using the Metropolis-Hasting MCMC method. A simulation example of capturing a tumbling satellite is provided to show the application and performance of the proposed method.

References

1. Flores-Abad, A., Ma, O., Pham, K., Ulrich, S.: A review of robotics technologies for on-orbit services. Progr. Aerospace Sci. **68**, 1–26 (2014)
2. Wee, L., Walker, M.W.: On the dynamics of contact between space robots and configuration control for impact minimization. IEEE Trans. Robot. Autom. **9**(5), 581–591 (1993)
3. Yoshida, K., Nenchev, D.N.: Space robot impact analysis and satellite-base impulse minimization using reaction null-space. In: IEEE International Conference on Robotics and Automation, pp. 1271–1277. Nagoya (1995)
4. Papadopoulos, E., Paraskevas, I.: Design and configuration control of space robots undergoing impacts. In: 6th International ESA Conference on Guidance, Navigation and Control Systems, pp. 17–20. Loutraki (2005)
5. Huang, P., Xu, Y.S., Liang, B.: Contac and impact dynamics of space manipulators and free-flying target. In: IEEE/RSJ International Conference on Intelligent Robots and Systems, pp. 382–337. Edmonton (2005)
6. Huang, P., Yuan, J., Xu, Y., Liu, R.: Approach trajectory planning of space robot for impact minimization. In: IEEE International Conference on Information Acquisition, pp. 382–387. Weihai (2006)
7. Huang, P., Liang, B., Xu, Y.S.: Configuration control of space robots for impact minimization. In: IEEE International Conference on Robotics and Biomimetics, pp. 357–362. Kunming (2006)
8. Dubowsky, S., Torres, M.: Path planning for space manipulators to minimize spacecraft attitude disturbances. In: IEEE International Conference on Robotics and Automation, pp. 2522–2528. Sacramento (1991)
9. Agrawal, O.P., Xu, Y.: On the global optimum path planning for redundant space manipulators. IEEE Trans. Syst. Man Cybern., 1306–1316 (1994)
10. Papadopoulos, E., Abu-Abed, A.: Design and motion planning for a zero-reaction manipulator. In: IEEE International Conference on Robotics and Automation, pp. 1554–1559. San Diego (1994)
11. Lampariello, R., Agrawal, S., Hirzinger, H.: Optimal motion planning for free-flying robots. In: IEEE International Conference on Robotics and Automation, pp. 3029–3035. Taipei (2003)
12. Aghili, F.: Optimal control for robotic capturing and passivation of a tumbling satellite with unknown dynamics. In: AIAA Guidance Navigation and Control Conference, pp. 1–21. Honolulu (2008)
13. Oki, T., Nakanishi, H., Yoshida, K.: Time-optimal manipulator control of a free-floating space robot with constraint on reaction torque. In: IEEE International Conference on Intelligent Robots and Systems, pp. 2828–2833. Nice (2008)
14. Walker, M.W., Wee, L.-B.: Adaptive control of space-based robot manipulators. IEEE Trans. Robot. Autom. **7**(4), 828–835 (1991)
15. Abiko, S., Hirzinger, G.: Adaptive control for a torque controlled free-floating space robot with kinematic and dynamic model uncertainty. In: IEEE/RSJ International Conference on Intelligent Robots and Systems, pp. 2359–2364 (2009)
16. Wang, H.: On adaptive inverse dynamics for free-floating space manipulators. Robot. Autonom. Syst. **59**(8), 782–788 (2011)
17. Xu, Y., You-Liang, G., Wu, Y., Sclabassi, R.: Robust control of free-floating space robot systems. Int. J. Control **61**(2), 261–277 (1995)
18. Pazelli, T.F., Terra, M.H., Siqueira, A.A.: Experimental investigation on adaptive robust controller designs applied to a free-floating space manipulator. Control Eng. Pract. **19**(4), 395–408 (2011)
19. Xu, G., Zhang, M., Wang, H.: Robust controller design for one arm space manipulator with uncertainties compensated. Lecture Notes Electr. Eng. Inf. Control Autom. Robot. Springer **133**(2), 59–66 (2012)
20. Chen, Z., Chen, L.: Robust adaptive composite control of space-based robot system with uncertain parameters and external disturbances. In: IEEE/RSJ International Conference on Intelligent Robots and Systems, pp. 2353–2358 (2009)
21. Aghili, F.: A prediction and motion-planning scheme for visually guided robotic capturing of free-floating tumbling objects with uncertain dynamics. IEEE Trans. Robot. Autom. **28**(3), 634–649 (2012)
22. Ma, O., Flores-Abad, A., Phan, K.: Control of a space robot for capturing a tumbling object international symposium on artificial intelligence. In: Robotics and Automation in Space. Turin (2012)
23. Flores-Abad, A., Wie, Z., Ma, O., Phan, K.: Optimal control of space robots for capturing a tumbling object with uncertainties. J. Guid. Control Dyn. **37**(6), 1–4 (2014)
24. Nanos, K., Papadopoulos, E.: On the use of free-floating space robots in the presence of angular momentum. Intel. Serv. Robot. **4**(1), 3–15 (2011)
25. Masutani, Y., Iwatsu, T., Miyazaki, F.: Motion estimation of unknown rigid body under no external forces and moments. In: IEEE International Conference on Robotics and Automation, pp. 1066–1072. San Diego (1994)
26. Xu, W., Liang, B., Li, C., Liu, Y., Xu, Y.: Autonomous target capturing of free-floating space robot: Theory and experiments. Robotica **27**, 425–445 (2009)
27. Aghili, F., Kuryllo, M., Okouneva, G., English, C.: Fault-tolerant position/attitude estimation of free-floating space objects using a laser range sensor. IEEE Sensors J. **11**(1), 176–185 (2011)

28. Petit, A., Marchand, E., Kanani, K.: Tracking complex targets for space rendezvous and debris removal applications. IEEE/RSJ Int. Conf. Intel. Robots Syst., 4483–4488 (2012)
29. Xu, Y., Kanade, T. (eds.): Space Robotics: Dynamics and Control. Kluwer Academic Publishers (1993)
30. Shah, S.V., Saha, S.K., Dutt, J.K.: Dynamics of tree-type robotic systems. In: Intelligent Systems, Control and Automation: Science and Engineering Bookseries. Springer, http://www.redysim.co.nr/ [cited September 17 2016.] (2013)
31. Hanßmann, H.: Quasi-periodic motion of a rigid body under weak forces. In: Hamiltonian Systems with Three or More Degrees of Freedom, pp. 398–402. Springer Netherlands (1999)
32. Kuang, J., Tan, S., Arichandran, K., Leung, A.Y.T.: Chaotic attitude motion of gyrostat satellite via Melnikov method. Int. J. Bifur. Chaos **11**(05), 1233–1260 (2001)
33. Masteron-Gibbons, M.: A Primer of the Calculus of Variation and Optimal Control Theory. American Mathematical Society, USA (2009)
34. Gilks, W.R., Richardson, S., Spiegelhalter, D.J.: Markov Chain Monte Carlo in Practice: Interdisciplinary Statistics. Chapman and Hall/CRC, London (1996)
35. Espero, M.T.: Future Space Robotics and Large Optical Systems: A Picture of Orbital Express. Ares V Workshop, California (2008)
36. Rutquist, P.E., Edvall, M.M.: Propt-Matlab Optimal Control Software. Tomlab Optimization Inc (2010)
37. Neal, R.M.: Suppressing random walks in Markov chain Monte Carlo using ordered overrelaxation. Learn. Graph. Models Springer **89**, 205–228 (1998)

Angel Flores-Abad received his Bachelor in Electronics Engineering from the Orizaba Institute of Technology, in 2004, Orizaba, Mexico; his MSc in Mechatronics Engineering from the National Center of Research and Technological Development, Cuernavaca, Mexico in 2007; and his PhD in Mechanical Engineering from New Mexico State University in 2013. Currently, he is in the Center for Space Exploration and Technology Research of the University of Texas at El Paso. His research interests include dynamics and control of space robotic systems and unmanned aerial vehicles.

Lin Zhang has completed his PhD program in Mechanical Engineering from New Mexico State University (NMSU). He is interests are Robotics, Biomechanics and Machine Learning. He is currently doing post-doctoral research about intelligent Robotics technology at NMSU.

Zheng Wei is currently a visiting assistant professor in Department of Mathematics and Statistics, University of Massachusetts Amherst. He graduated from New Mexico State University and received his Ph.D. in Mathematics in 2015. His research interest includes the multivariate analysis, Bayesian statistical methods for big data, the copula theory and random set theory.

Ou Ma received a B.S. degree in 1982 from Zhejiang University and an M.S. and Ph.D. degrees from McGill University in 1997 and 1991, respectively. He is now an endowed chair professor in the Department of Mechanical and Aerospace Engineering, New Mexico State University (NMSU). His research interests are in design, dynamics, and controls of space robotic systems and unmanned aerial vehicle systems. He is currently supervising the Reduced-Gravity and Biomechanics (RGB) Lab, the Advanced Robotics Lab, and the Mechatronics/UAV Lab of NMSU. From 1991 to 2002, Dr. Ma worked as an R&D lead and senior project engineer for MDA Robotics and Automation (then called MDA Space Missions), Brampton, Canada, participated in operation support of the Space Shuttle Remote Manipulator System (Canadarm), and development of the Space Station Remote Manipulator System (Canadarm2) and Special Purpose Dexterous Manipulator (Dextre) for the Canadian Space Agency. He also participated in the development of the European Proximity Operation Simulator (EPOS) for the German Aerospace Center. Dr, Ma has published over 150 papers in major robotics and aerospace journals and conferences and owned many patents.